Trace elements in clinopyroxenes from Aleutian xenoliths: Implications for primitive subduction magmatism in an island arc

G.M. Yogodzinski [a,*], P.B. Kelemen [b,1]

[a] *Department of Geological Sciences, University of South Carolina, 701 Sumter St., EWSC617, Columbia, SC 29208, United States*
[b] *Lamont-Doherty Earth Observatory, Palisades, NY 10964, United States*

Abstract

Trace element abundances in clinopyroxene (cpx) from cumulate xenoliths are used to characterize the nature of primitive magma-forming processes beneath the Aleutian island arc. Clinopyroxenes from deformed mafic and ultramafic xenoliths hosted in a Neogene-age mafic sill from Kanaga Island have widely varying trace element abundances (Sr=8–32, Y=2–64, Zr=2–38, Nd=0.65–16 ppm) that are generally well correlated with cpx Mg# (Mg/Mg+Fe). Trace element ratios in the Kanaga xenoliths show relatively little variability (Nd/Yb=1.7–3.5, Sr/Y=0.20–8.7, Nd/Zr=0.10–0.43) and trace element patterns are generally parallel to one another, with the most evolved samples showing pronounced negative Eu anomalies (Eu/Eu*=0.56–0.66). In contrast, cpx from xenoliths hosted in Holocene-age pyroclastic deposits from Mt. Moffett on Adak Island, have more strongly fractionated trace element patterns, with higher and more variable Sr (8–69 ppm), Nd/Yb (3.1–10.5) and Sr/Y (0.5–47) compared to Kanaga xenolith cpx. Clinopyroxene from the amphibole-bearing and igneous-textured Moffett xenoliths also lack substantial negative Eu anomalies (Eu/Eu*=0.84–1.25). With respect to most trace element characteristics, cpx from the Kanaga xenoliths resemble cpx phenocrysts from Aleutians basalts, and are distinct from Moffett xenolith cpx which resemble phenocrysts from primitive and geochemically enriched, high-Mg# andesites. The strongly contrasting trace element patterns in the two xenolith suites, which are most clearly evident in the most primitive samples (cpx Mg#>0.86), are present in cpx with broadly similar major element characteristics (XWo=0.40–0.50, XCaTs=0.02–0.25, Mg#=0.65–0.92), and are interpreted to result from differences in the trace element characteristics of the primitive melts that crystallized to produce the xenoliths. Melts that crystallized to produce the Kanaga xenoliths appear to have been similar to modern Aleutian basalts, whereas those that produced the Moffett samples were more hydrous and perhaps more oxidized and had more strongly fractionated trace element patterns, analogous to those observed in the geochemically enriched primitive andesites. If the trace element-enriched signature in the Moffett xenoliths is produced by melting of the subducting plate in the presence of garnet, then these results support recent thermal modeling which suggests that a 50–60 m.y.-old subducting plate, such as that beneath the central Aleutians, may commonly reach at least those temperatures required to produce eclogite melting under water-saturated conditions (~850 °C). These results indicate that primitive melts arising from the subduction zone are geochemically diverse and may exert primary control over the nature of the distinctive igneous differentiation series (calc–alkaline versus tholeiitic) which are observed in Aleutian volcanoes.
© 2007 Elsevier B.V. All rights reserved.

* Corresponding author. Tel.: +1 803 777 9524; fax: +1 803 777 4352.
E-mail addresses: gyogodzin@geol.sc.edu (G.M. Yogodzinski), peterk@ldeo.columbia.edu (P.B. Kelemen).
[1] Tel.: +1 845 365 8728; fax: +1 845 365 8155.

1. Introduction

Subduction systems exert first-order controls over the nature of crust–mantle recycling, and play a major role in the evolution of the solid-earth geochemical system [1,2]. To a large degree our understanding of the physical and chemical conditions in subduction zones comes from geochemical studies of island arc lavas, especially lavas that are primitive (relatively Mg/Mg + Fe, or Mg#) and have therefore been little-modified by shallow processes (e.g., [3–5]). Most arc lavas are however, evolved (whole-rock Mg# < 0.60), and have been substantially modified by crystal fractionation, mixing and/or assimilation in relatively shallow, crustal-level magma chambers (e.g., [6]). These processes commonly obscure the mantle-level processes that underlie magma genesis in subduction zones.

An alternative approach to understanding subduction magmatism, one that is largely independent of observations of arc lavas, is through the petrologic and geochemical study of mafic and ultramafic xenoliths from modern subduction systems. Such studies are relatively rare because subduction-related xenoliths are rare, however where they exist, mafic and ultramafic xenoliths provide an important source of information on the physical and chemical conditions in subduction zones (e.g., [7–13]).

Here, we present new trace element analyses of clinopyroxene (CPX) from mafic and ultramafic xenoliths from Adak and Kanaga islands in the central Aleutian Island arc (Fig. 1). These data demonstrate that variability of key trace element concentrations and ratios (Sr, Nd, Nd/Yb, Sr/Y) is greatest in Aleutian xenolith CPX with Mg#'s > 0.86. The highly variable trace element contents of these primitive CPX converge on relatively uniform, 'normal' compositions in evolved CPX at moderate-to-low Mg-number (< 0.80). These observations are consistent with previous studies of CPX phenocrysts in primitive Aleutian lavas [14], and with the idea developed through whole-rock studies, that melts arising from the Aleutian sub-arc mantle are themselves enormously diverse, ranging in composition from arc basalts and picrites with 'normal' subduction-related trace element enrichments compared to MORB, to primitive andesites with highly enriched trace element patterns [3,15–19], now often referred to as 'adakites' [20]. The data presented here are discussed in the context of geochemical source components, with an emphasis on understanding the physical conditions and geochemical processes that have contributed to the genesis of lavas produced in the Aleutian subduction system.

2. Xenolith locations, petrography and mineralogy

Xenoliths selected for this study are from Kanaga and Adak islands in the central part of the Aleutian island arc (Fig. 1). At the Kanaga location, the xenoliths are hosted by basaltic sills and dikes, which intrude rocks of probable Neogene age [21–24]. On Adak, the xenoliths occur in Holocene-age pyroclastic deposits from Mt. Moffett [7,10,25]. All samples have been well characterized
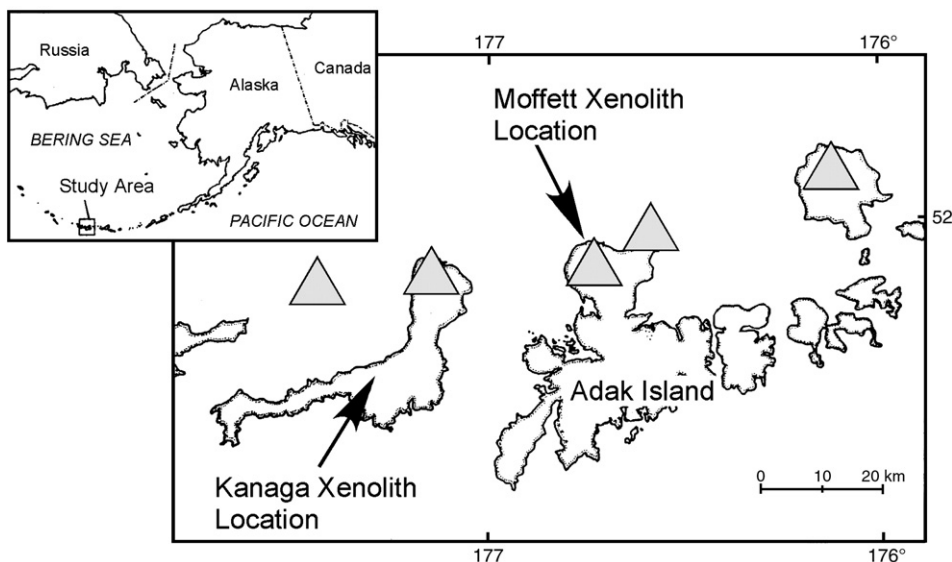

Fig. 1. Location map. Xenoliths discussed in this paper are from Kanaga and Adak Islands in the central Aleutian arc (see inset). Large, gray triangles show the locations of the late Pleistocene and Holocene volcanoes Bobrof, Kanaga, Moffett, Adagdak, and Great Sitkin (west-to-east).

through previous electron probe, petrographic and whole-rock geochemical work [7,10,22,24–27]. A key outcome of this prior work is that the Kanaga and Moffett xenoliths formed in Aleutian magma chambers, and that they are not fragments of depleted arc mantle. This conclusion is based primarily on the pyroxene-rich mineralogy of the specimens, the widely variable Mg# of olivine and pyroxene indicating crystallization from melts at widely variable temperatures, and the presence of complex compositional zoning within minerals, indicating an important role for magma mixing in some samples [7,22]. The implication of this prior work is that xenoliths with primitive CPX (Mg#>0.86) contain information on magmatic processes that occur at deeper levels and higher Mg#'s than are generally captured in whole-rock studies of Aleutian lavas [7,10,22,25]. We use the term 'primitive' in this context, because CPX with Mg#'s from 0.86 to 0.92 have compositions which may be in equilibrium with mantle olivine (Mg#=0.88–0.93), based a K_D=1.2 for Fe–Mg exchange between olivine and CPX in Mg-rich magmas [28].

Included among the Kanaga xenoliths (Table 1) are samples with ultramafic compositions, but most contain a considerable quantity of plagioclase, and have variable compositions between olivine-bearing and two-pyroxene gabbros [21,22,24,27]. A few of the Kanaga xenoliths retain gabbroic (igneous) textures, but most are strongly-deformed, and typically show sutured and irregular grain boundaries, kink-banding, fractured grains, and undulose extinction. Texturally, the deformed samples are relatively fine grained and equi-

granular (granoblastic textures), but the presence of large relict crystals (porphyroclasts) in some samples suggests that the rocks have undergone grain-size reduction from an originally coarse (3–8 mm) texture [21,22,24].

The xenoliths from Mt. Moffett (Adak Island, Fig. 1, Table 1) are coarse-grained plutonic rocks that retain cumulate and other igneous textures [7,25]. These xenoliths include (1) cumulate-textured, amphibole-bearing olivine pyroxenites and gabbros, (2) cognate inclusions with coarse (megacrystic) olivine, CPX, and amphibole, and (3) 'composite' xenoliths, which are interpreted on textural grounds to be inclusions of crystal-rich primitive melts that were quenched and solidified prior to being incorporated into the host magma [7,25]. The presence of amphibole in the Moffett xenoliths, which is observed to be a late-crystallizing/intercumulus phase in many samples, distinguishes the Moffett xenoliths from those at Kanaga, which contain no hydrous primary minerals [7,25].

Clinopyroxenes from the Moffett and Kanaga xenoliths are broadly alike in their major element compositions [7,22]. Relict/unrecrystallized CPX in the Kanaga xenoliths [22] vary continuously from diopside to salite and calcic augite, defining a relatively narrow range of Ca contents (Wo_{39-50}) over a wide range in Fe and Mg (CPX Mg#=0.65–0.90). The Al_2O_3 contents of CPX in the Kanaga samples are usually 2–5 wt.%, but in some samples are as high as 7.5–8.5%. The Ca-Tschermaks component, which reflects the Al_2O_3 content and may significantly influence the partitioning of trace elements in CPX [29,30], is consequently low in most Kanaga

Table 1
General features of Kanaga and Moffett xenoliths

Sample no.	Rock type	Mineralogy [a]	Texture	Average grain size (mm)	References
KAN80-6-76	Olivine-bearing gabbro	plag, cpx, olv	Gabbroic	3–4	[22]
KAN80-6-89	Two-pyroxene gabbro	plag, cpx, opx	Granoblastic	1–2	[22]
KAN80-7-41	Olivine-bearing gabbro	plag, cpx, olv	Granoblastic	<1	[22]
KAN80-7-2	Olivine-bearing gabbro	cpx, plag, olv	Granoblastic	<1	[22]
KAN80-7-22	Gabbro	plag, cpx	Granoblastic	1–2	[22]
KAN80-7-24	Two-pyroxene gabbro	plag, cpx, opx	Gabbroic	2–3	[22]
KAN80-7-39	Gabbro	plag, cpx	Granoblastic	1–2	[22]
KAN80-6-11	Werhlite	olv, cpx	Granoblastic	1–2	[24]
KAN80-6-69	Werhlite	olv, cpx	Granoblastic	2–3	[24,27]
KAN80-6-5	Werhlite	olv, opx, cpx	Granoblastic	1–2	[24,27]
MM77-102 [b]	Olivine clinopyroxenite	olv, cpx, amph	Cumulate	2–3	[7,10,25]
MM77-102A [b]	Olivine clinopyroxenite	olv, cpx, amph	Cumulate	2–3	[7,25]
MM77-102C [b]	Olivine clinopyroxenite	olv, cpx, amph	Cumulate	2–3	[7,25]
MM77-43	Amphibole clinopyroxenite	olv, cpx, amph	Cumulate	1–2	[7,25]
MM79A	Megacryst in basaltic andesite	cpx	–	5–6	[7,25]
MMDK	Hornblende gabbro	plag, cpx, amph, olv	Gabbroic	2–4	[7,10,25]

[a] Mineral abbreviations are olv (olivine), cpx (clinopyroxene), amph (amphibole), opx (orthopyroxene) and plag (plagioclase).
[b] Sample 102, 102A and 102C are separate thin sections of one large xenolith.
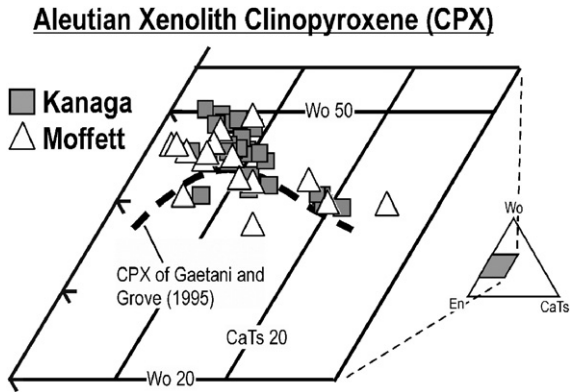
Aleutian Xenolith Clinopyroxene (CPX)

Fig. 2. Major element compositions of clinopyroxene (CPX) from Aleutian xenoliths and from experimental work of Gaetani and Grove [29], plotted in terms of the wollastonite (WO), enstatite (EN) and Ca-Tschermaks (CaTs) pyroxene components. Similar compositions among the Aleutian samples, especially with respect to the WO and CaTs components, suggest that CPX/melt partitioning of trace elements at the Kanaga and Moffett locations will be broadly similar. Bold, dashed line shows the locations of CPX of Gaetani and Grove [29]. These data are from Conrad and Kay [7] and Romick [22].

xenolith CPX (XCaTs < 0.10) but varies to relatively high values in samples with high Al_2O_3 (XCaTs up to 0.25; Fig. 2). Clinopyroxenes from the Moffett xenoliths [7] span nearly the same compositional range as the Kanaga xenolith CPX, extending only to slightly higher Al_2O_3 contents (up to 10%) and equivalently higher Ca-Tschermaks component compared to the Kanaga samples (Fig. 2). The range of Ca-Tschermaks component in

Aleutian xenolith CPX is similar to that in Gaetani and Grove's [29] experimental study of trace element partitioning in CPX (Fig. 2).

The primary difference between CPX in the Kanaga and Moffett xenoliths is that Kanaga CPX compositions are relatively uniform within samples, and are substantially free of core-to-rim compositional zoning [22]. In contrast, the Moffett CPX from some xenoliths show complex and fine-scale zoning that is clearly evident petrographically, and shows strong oscillatory patterns of normal and reverse shifts in Fe/Mg from core to rim [7]. This pattern is well illustrated by a core-to-rim microprobe traverse of a CPX crystal from composite xenolith sample MOF77-43 (Fig. 3). These textural-compositional differences in CPX from xenoliths of the different groups, probably reflect in-part, annealing and diffusive equilibration of the Kanaga xenoliths during metamorphism and storage in the Aleutian crust since at least the Neogene, compared to the undeformed plutonic–volcanic textures seen in the Moffett xenoliths which were carried to the surface in the Holocene and appear to be related to modern magmatic processes [7,25].

3. Results: trace elements in xenolith clinopyroxene

Trace element concentrations were measured by ion microprobe on representative CPX crystals selected from four xenolith samples from the Moffett location and ten from the Kanaga location. This selection reflects
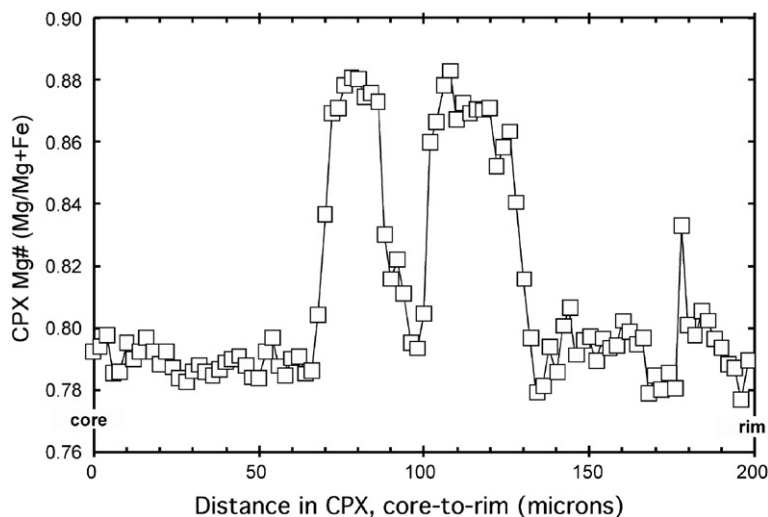

Fig. 3. Mg# (Mg/Mg + Fe) in clinopyroxene (CPX) from Aleutian xenolith #77-43 from the Moffett location, illustrating the results of a 200-micron electron probe traverse through a strongly zoned portion of a single CPX crystal. The CPX analyzed to produce these results is texturally and compositionally similar to the one illustrated in Fig. 4 of Conrad and Kay [7], also from sample #77-43. Analyses are spaced at 2-micron intervals. Compositional oscillations such as these (jumps of Mg# = 0.79 to 0.87 over distance of less than 6–10 μm) are common in 'composite' xenolith CPX from the Moffett location (see also Fig. 4 in [7]).

the number of samples available from the different locations and the amount of prior whole-rock, petrographic and electron probe work that has been done. In-situ 'spot' analyses were made on from 1-to-4 CPX crystals from each sample. The total number of spot analyses per sample reflects the degree of geochemical variability that was observed as the data were collected. The measurements were made using the Cameca 3f ion microprobe at the Woods Hole Oceanographic Institution, following the methods of Shimizu [31]. Operating conditions used for data collection in this study are summarized in Yogodzinski and Kelemen [14].

Kanaga xenolith CPX have concentrations of Zr, Y, Nd, Yb and other strongly-to-moderately incompatible trace elements, that are highly correlated with one another and are inversely correlated with CPX Mg-number (Figs. 4, 5). In contrast, Kanaga xenolith CPX show no systematic variation in the abundance of Sr (a moderately compatible element) over a wide range of incompatible element concentrations or CPX Mg-number (Figs. 4, 5). Concentrations of the strongly compatible element Cr, are in general positively correlated with CPX Mg-number, and show inverse relationships with Zr, Nd, Y and other incompatible elements (Table 2). Rare-earth element patterns in Kanaga xenolith CPX are generally smooth and parallel to one another over a wide range of abundances, and show pronounced negative Eu-anomalies in the most evolved samples (i.e., low Eu/Eu* at high Nd and Yb and low CPX Mg-number; Fig. 6). Europium anomalies in the Kanaga xenoliths are not however, correlated with the general shape of the REE patterns in CPX as
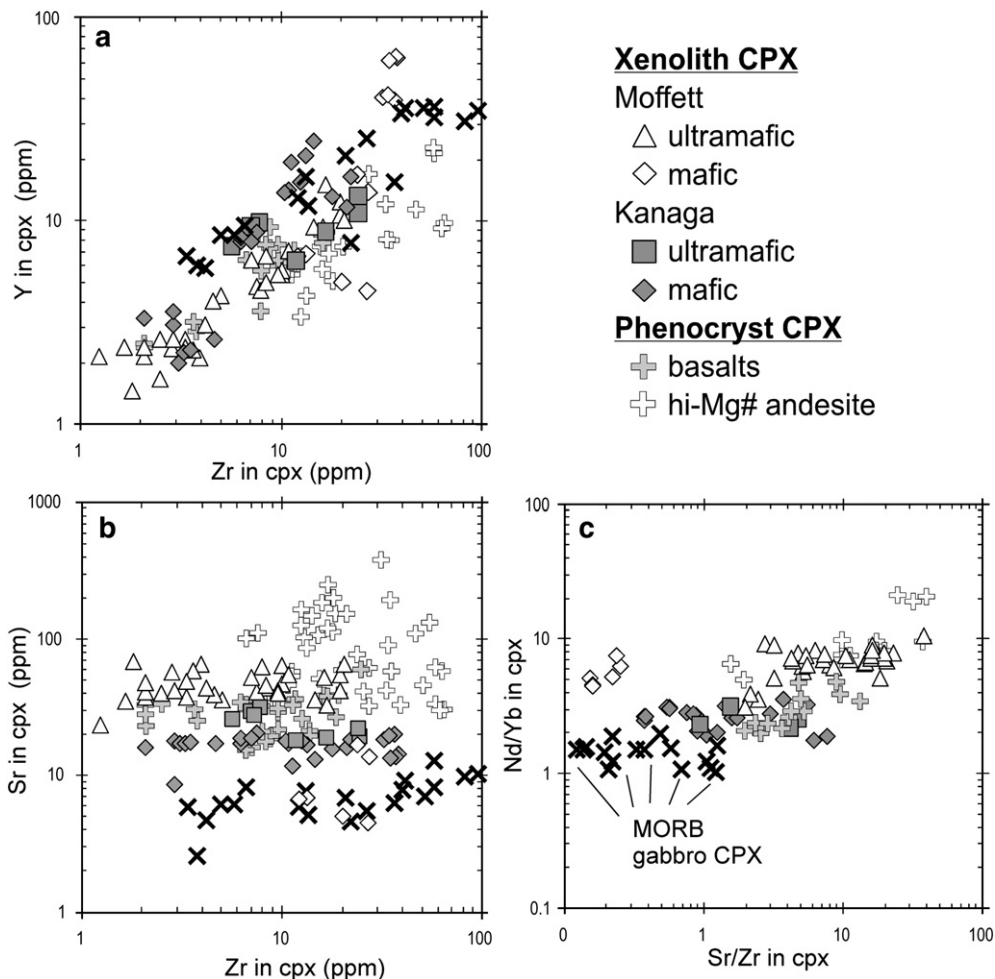

Fig. 4. Trace element abundances (Y, Sr, Zr) and ratios (Nd/Yb, Sr/Zr) in clinopyroxene (CPX) from Aleutian xenoliths compared with CPX from MORB gabbros and phenocrysts in primitive Aleutian lavas. Plagioclase is present in the mafic, but not the ultramafic xenoliths. Data from the Kanaga and Moffett xenoliths are from Tables 2 and 3. Aleutian phenocryst data are from Yogodzinski and Kelemen [14]. MORB gabbro data are from Dick and Naslund [83].
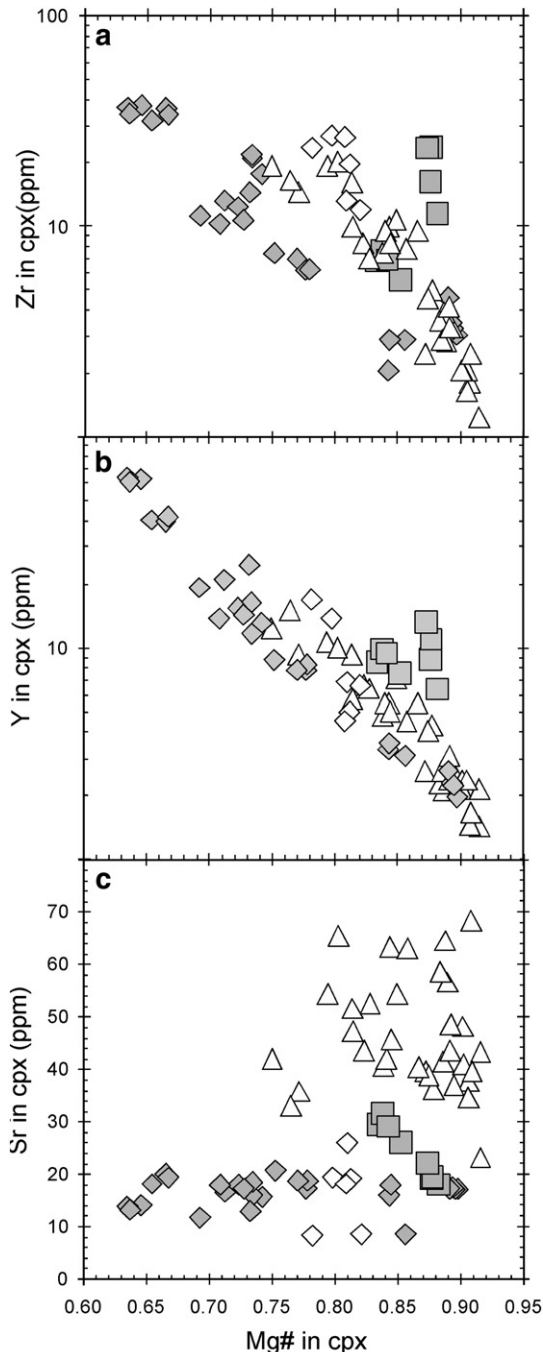
Fig. 5. Trace element abundances (Zr, Y, Sr) in clinopyroxene (CPX) from Aleutian xenoliths, plotted again CPX Mg# (Mg/Mg+Fe). Symbols and data sources are as in Fig. 4.

indicated for example by Nd/Yb. Overall, the trace element characteristics of the Kanaga xenolith CPX are readily distinguished from those in CPX from MORB gabbros, but closely resemble those of CPX phenocrysts in primitive Aleutian basalts (Figs. 4, 6, 7).

Trace elements in Moffett xenolith CPX illustrate most of the same types of variation as do the Kanaga CPX (i.e., incompatible trace elements are well correlated with each-other and inversely correlated with compatible trace elements and with CPX Mg-number — Figs. 4, 5). There are however important differences in trace elements between Moffett and Kanaga CPX. These differences are clearest in Sr and Nd abundances, and in Nd/Yb, Sr/Y, Sr/Z and Nd/Zr which are systematically higher in the Moffett samples than Kanaga (Figs. 4, 7). The contrast between the CPX from the Kanaga and Moffett locations is also well illustrated by the REE patterns, which are less strongly depleted in light rare-earth elements at the Moffett location, and lack the prominent Eu anomalies that are present in some Kanaga samples (Fig. 6). Individual CPX crystals in the Moffett xenoliths are also far more variable in the REE abundances than are CPX from the Kanaga xenoliths, which are largely uniform within samples (Fig. 6a). Perhaps most importantly, the differences in trace elements between the Moffett and Kanaga CPX are greatest at high Mg-number (>0.86), and converge toward similar values at low Mg-number (<0.80). This relationship is particularly clear in plots Sr, Nd, Sr/Y, Nd/Yb and Nd/Zr against CPX Mg-number (e.g., Figs. 4, 7). The only clear exception to the rule that these CPX populations are different is the singular plagioclase-bearing/gabbroic sample (MM-DK) which has low Sr and low Sr/Y compared to all other samples from the Moffett location.

4. Discussion

4.1. Genesis of the Aleutian xenoliths

The data presented above clearly separate the Kanaga and Moffett CPX populations on the basis of trace element geochemistry. The broad similarity in major element compositions of these CPX (Fig. 2) implies that the strong differences in their trace element contents (Figs. 4–7) must reflect, to a large degree, the contrasting trace element compositions of the melts that produced them, and cannot be (primarily) the product of crystal fractionation from a common parental melt, or of crystal–chemical controls over trace element partitioning that may have effected one CPX population but not the other. This is particularly clear for the rare-earth elements, which according to the partitioning data of Gaetani and Grove [29] may vary by 40% in Ce/Yb for CPX with Ca-Tschermaks in the range observed in the Kanaga and Moffett samples (Fig. 2). This crystal–chemical effect is significant but small compared to the average factor-of-

Table 2
Trace element analyses of clinopyroxenes from Kanaga Island xenoliths

Sample no.	KAN80-6-76	KAN80-6-76	KAN80-6-89	KAN80-6-89	KAN80-7-41	KAN80-7-41	KAN80-7-2	KAN80-7-22	KAN80-7-24	KAN80-7-39	KAN80-6-11	KAN80-6-69	KAN80-6-5
Analysis no.	1	3	3	4	1	3	Average (n=3)				(n=4)		
Mg#	0.86	0.84	0.63	0.64	0.72	0.71	0.77	0.74	0.71	0.66	0.89	0.84	0.88
Ti	1463	1616	2843	2687	2644	2680	1456	1121	2129	2666	1230	3323	2904
V	264	360	413	372	471	511	387	323	534	387	181	382	285
Cr	1020	1181	96	80	989	793	2712	503	48	144	3401	1944	3237
Sr	8.7	17.9	13.9	13.3	17.9	17.9	18.9	16.8	13.8	19.3	17.3	29.2	19.8
Y	3.09	3.57	63.8	61.2	15.5	13.8	8.21	13.7	21.6	40.5	2.29	8.89	9.89
Zr	2.92	2.92	37.1	34.6	12.5	10.4	6.78	20.4	13.1	34.3	3.64	6.83	19.0
La	0.12	0.12	1.73	1.52	0.68	0.54		0.94	0.46	1.42	0.17	0.28	0.34
Ce	0.52	0.57	10.08	8.40	3.17	2.52		3.56	2.70	7.71	0.68	1.21	1.53
Nd	0.89	0.74	15.8	13.9	4.36	3.58		3.70	4.68	11.4	0.78	1.74	2.02
Sm	0.43	0.47	7.88	6.31	2.11	1.77		1.76	2.59	5.42	0.38	0.91	0.88
Eu	0.15	0.21	1.81	1.22	0.62	0.60		0.62	0.55	1.24	0.15	0.40	0.37
Dy	0.56	0.89	11.52	8.18	2.82	2.42		2.47	3.60	6.76	0.53	1.43	1.47
Er	0.37	0.42	6.61	4.46	1.43	1.36		1.29	2.02	3.80	0.22	0.75	0.79
Yb	0.32	0.42	6.35	5.22	1.39	1.38		1.33	2.32	3.72	0.23	0.73	0.78
Nd/Yb	2.79	1.75	2.48	2.65	3.14	2.60		2.78	2.02	3.07	3.41	2.39	2.61
Sr/Y	2.80	5.02	0.22	0.22	1.16	1.30	2.31	1.22	0.64	0.48	7.56	3.28	2.00
Nd/Zr	0.31	0.25	0.43	0.40	0.35	0.34		0.18	0.36	0.33	0.22	0.25	0.11

three difference in CPX Ce/Yb between the Kanaga (Ce/Yb ~ 2.0) and Moffett (Ce/Yb ~ 6.3) samples.

The Moffett and Kanaga CPX overlap broadly at high Mg# > 0.86, indicating that the melts that crystallized these pyroxenes were similar with respect to Fe/Mg and primitive enough to have been in equilibrium with mantle olivine with forsterite contents of 0.88–0.93 [28]. We emphasize however that the melts that produced these pyroxenes need not have been similarly hot or similar in their volatile or SiO_2 content, or fO_2. We recognize that differences in temperature, melt structure and fO_2 (in addition to crystal–chemical effects) may significantly influence trace element partitioning in pyroxenes (e.g., [29]). Given their differences in trace element contents, it seems certain that the volatile content and structure of the melts that formed the Moffett and Kanaga CPX were also systematically different. These likely but unquantified differences serve primarily to underscore the main point (elaborated below), which is that the primitive melts that produced these CPX were fundamentally different from one another and probably formed by different petrogenetic processes.

Distinctions between CPX from the Kanaga xenoliths and MORB gabbros, which are particularly evident in Sr/Y, Nd/Yb, Nd/Zr, Sr and Nd (Figs. 4–7), are clearly analogous to the contrasting trace element patterns seen in whole-rock data from arc lavas compared to MORB. These differences in trace element abundances and inter-element ratios in CPX from the Kanaga xenoliths are distinct from those in MORB gabbros in ways that are consistent with the idea that these xenoliths are related to the genesis of primitive Aleutian melts [22]. Based on their overall geochemistry, which overlaps broadly with CPX phenocrysts in Aleutian basalts (Figs. 4, 7), we conclude that the Kanaga xenolith CPX formed by crystallization and crystal fractionation processes involving Aleutian basaltic melts in the Neogene. This conclusion is consistent with whole-rock studies of the Kanaga xenoliths, which have emphasized that they formed primarily as cumulates derived from evolving basaltic melts [22].

In contrast, CPX from the Moffett xenoliths have relatively enriched trace element patterns (higher Sr/Y, Nd/Yb) that are unlike those seen in CPX phenocrysts in Aleutian basalts, but are like those seen in phenocrysts from the primitive and geochemically enriched high-Mg# andesites (Figs. 4, 7). The geochemical diversity in CPX at high Mg# in the Moffett xenoliths, which is similar to the variation in CPX phenocrysts in Aleutian lavas [14], underscores the point that Aleutian primitive lavas are already compositionally diverse when they pass from the mantle into the crust. This is an important point, because some aspects of arc volcanism, in particular the enriched REE patterns that are commonly observed in calc–alkaline andesites compared to arc basalts [e.g.,
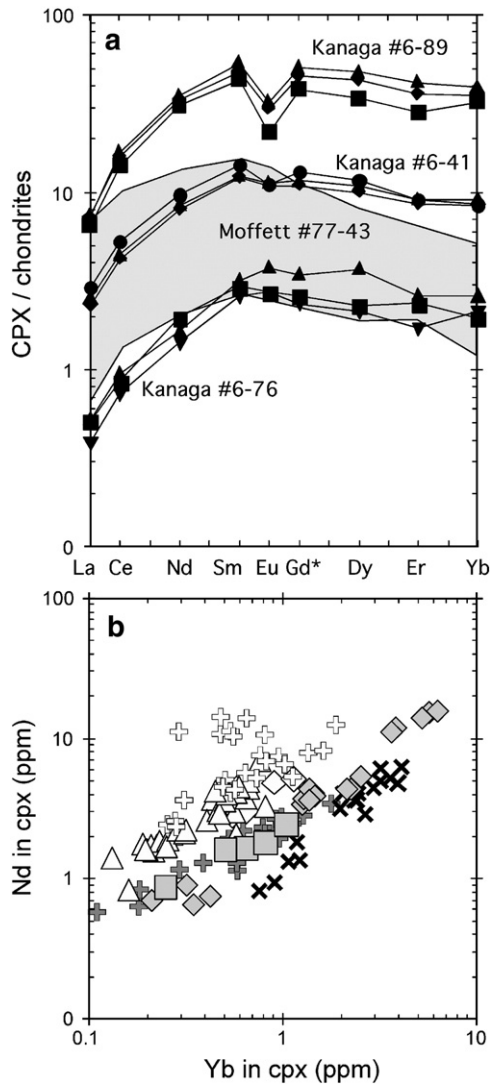
Fig. 6. Rare-earth element (REE) variation in Aleutian xenolith and phenocryst CPX compared with CPX from MORB gabbros. Data sources are as in Fig. 3. (a) shows the compositions of separate CPX crystals within three individual xenolith samples from Kanaga (6–89, 41, 76) compared to the range of CPX compositions in one Moffett sample (77-43, gray field). (b) shows the strong positive variation between Nd and Yb, emphasizing the higher Nd/Yb in the Moffett compared to Kanaga samples. Data symbols in (b) are as in Fig. 3.

crystallization [28]. Similarly, the trend of decreasing Sr/Nd, Nd/Yb and Nd/Zr, and decreasing trace element variability with decreasing Mg#, is the opposite of that predicted for crustal melting and magma mixing or assimilation [14,19], indicating again, that these
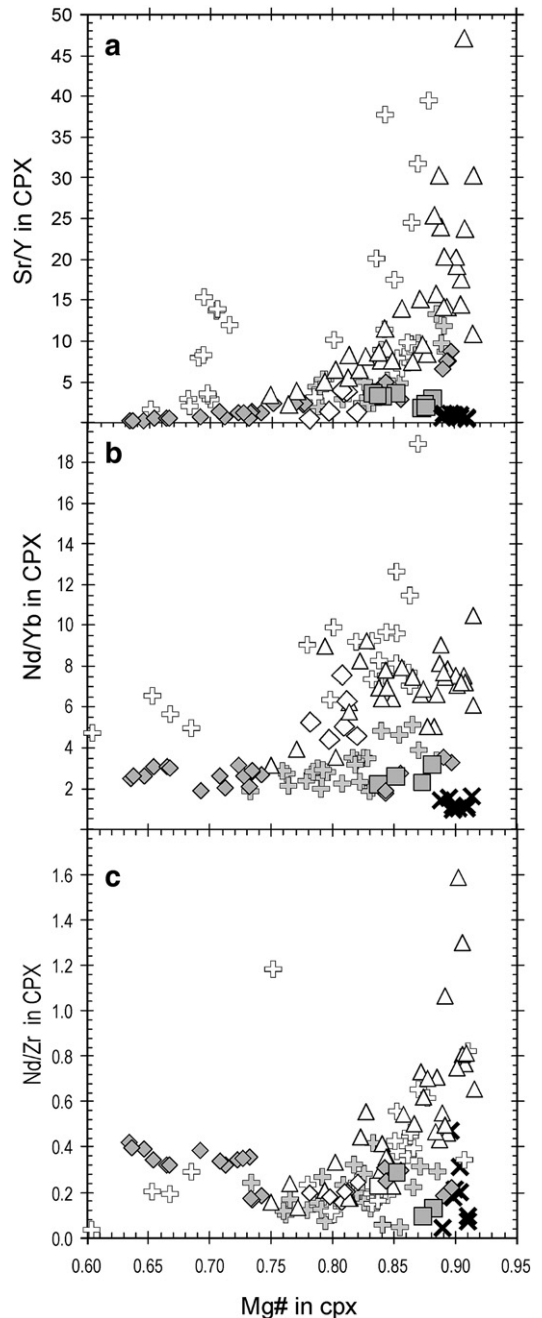

Fig. 7. Trace element ratios (Sr/Y, Nd/Yb, Nd/Zr) in clinopyroxene (CPX) from Aleutian xenoliths, phenocrysts and MORB gabbros plotted again CPX Mg# (Mg/Mg + Fe). Symbols and data sources are as in Fig. 4.

Fig. 13 in [32], Fig. 19 in [33]], are often attributed to magma mixing, crustal melting and assimilation, or to crystal fractionation involving amphibole or other minerals capable of fractionating the light from the heavy REE's (e.g., [32]). The presence of high Sr/Y, Nd/Yb, etc., at high Mg# in the Moffett CPX (0.86–0.92) implies that these enriched trace element features were present in melts that may have been in equilibrium with olivine in mantle peridotite prior to the onset of amphibole

enriched trace element characteristics were present in samples that arose from the Aleutian mantle wedge.

The presence of high Sr/Y and Nd/Yb primarily in CPX with high Mg#'s, and the general decline in these trace element ratios in CPX with low Mg#'s (Fig. 7), are consistent with the idea that the high Sr/Y geochemical component, which we interpret to be an eclogite-melt component from the subducting plate, makes up a volumetrically small proportion of the source of Aleutian magmas, and that its fractionated trace element pattern is commonly diluted by larger-scale melting and melt-rock reaction within the mantle wedge, and/or by the pooling and homogenization of diverse melts within the deep crust and upper mantle [18,19]. The same inverse pattern of declining Sr/Y and Mg# (Fig. 7) is also observed in trace element data from CPX phenocrysts, and has been interpreted to result from the mixing of geochemically enriched primitive andesite with common magma types which are more voluminous and have 'normal' trace element patterns [14].

Based on the above, we conclude that the Kanaga and Moffett xenoliths were produced through magma chamber processes beginning with primitive melts that were geochemically distinct from one another in approximately the way the primitive basalts of the modern arc are distinct from the geochemically enriched primitive andesites. These observations underscore conclusions reached through whole-rock studies of Aleutians lavas, which have emphasized that primitive melts arising from the mantle wedge vary continuously from basalts and picrites that have relatively flat trace element patterns, to geochemically enriched andesites that are relatively hydrous and oxidized, and have strongly fractionated trace element patterns compared to those of common arc basalts. This view of arc magmatism, which has evolved out of the unique existence of widespread high-Mg# andesite-related magmatism in the western Aleutians [18,19,33], is closely mirrored in the well studied primitive lavas of the Mt. Shasta area (northern California) which similarly vary in composition from nearly anhydrous basalts with flat trace element patterns, to basaltic andesites and andesites that have fractionated trace element patterns and primitive isotopic compositions [34–39].

4.2. Nature of the slab component beneath the Aleutians

If it is true that the Moffett xenoliths are the product of enriched, high-Mg# andesite magmatism, and that this style of magmatism originates as a partial melt of subducting basalt in the eclogite facies [16,18–20,40], then we may also conclude that the subducting plate beneath the Adak area was hot enough to melt beneath the Aleutian arc at the time the Moffett xenoliths formed. This result is perhaps surprising, because the Pacific Plate that is presently entering the trench off of Adak Island is ∼50–60 m.y.-old, and has not been more than 40–60 m.y.-old over the past 15 Ma [19,41,42]. The presence of an eclogite melt in this context is unexpected, because many thermal models of subduction zones predict melting of the slab only when the subducting oceanic lithosphere is exceptionally young (e.g., [43–46]). The presence of an eclogite melt component in the Moffett xenoliths is however, consistent with recent thermal models which incorporate temperature-dependant and/or non-Newtonian viscosity [47–50]. These models predict slab-surface temperatures that are 100°–300° hotter than the older models, and in general, they are in better agreement with a variety of observations, especially regarding the PT conditions in arc lower crust and mantle wedge [see discussion in [48,50]]. If the recent thermal models are correct, or if they are at least more correct than the older models, then there is good reason to believe that eclogite melts may be common beneath the Aleutians, and therefore may have played a role in the genesis of the Moffett xenoliths, as indicated by our trace element data.

Recent experimental studies also suggest that eclogite melting may be a common process in subduction zones. In particular, the work of Schmidt et al. [51] demonstrates that greywacke, pelagic sediment and basalt all have essentially identical H_2O-saturated solidus temperatures under eclogite conditions [see also [52–55]]. This is important, because there is strong evidence that subducted sediment is nearly always incorporated into the source of arc lavas in the form of a melt [56–62]. The petrologic similarity of basalt and sediment under eclogite conditions, which is clearly implied by the experimental studies of Schmidt et al. [51] and others, therefore indicates that if sediment melts are nearly always present in subduction zones [58], then melts from subducted basalt should commonly be present as well.

Finally, we note that the recent experiments of Kessel et al. [63,64] have demonstrated that at 5–6 GPa, the properties of slab-derived hydrous fluids and silicate melts merge into a supercritical liquid that has solubilities for most of the important trace elements which are indistinguishable from those of eclogite melts. If the slab component beneath the Aleutians is derived from the subducting plate in this pressure range, then the supercritical liquid like the one observed by Kessel et al.

[63], would provide an alternative source for the enriched trace element geochemistry observed in CPX from the Moffett xenoliths. This 'super-critical liquid' would be indistinguishable from an eclogite melt component on the basis of its trace element characteristics [63], but distinct from the 'aqueous fluids' which have been characterized in a variety of experimental studies [65–67], and which are widely believed to play a key role in controlling the trace element patterns of island arc lavas (e.g., [4,68]).

One assumption implicit in the above discussion is that the Moffett xenoliths are themselves young, and that they therefore have formed in the modern tectonic setting of the central Aleutians, or in a similar setting within the recent past (<6 Ma). If on the other hand, the Moffett xenoliths are many millions of years old, then their genesis could be a product of poorly understood Miocene or older events such as ridge subduction [69].

Conrad and Kay [7] pointed out that 'composite' xenoliths from Mt. Moffett (e.g. #77-43, Table 3) have volcanic textures, with large, phenocrystic amphibole, olivine and pyroxene set in a fine matrix of plagioclase laths and glass that is texturally and modally distinct from the matrix of the host material. These observations led Conrad and Kay [7] to interpret these xenoliths as mixed-and-mingled primitive melts that were quenched and partially solidified prior to incorporation into the host melt, which erupted in the Holocene. These relationships suggest that the xenoliths are not acciden-

tal fragments of ancient country rocks, but were part of the active magma generation processes beneath Mt. Moffett in the Holocene [7]. If, as we have argued, the trace element characteristics of CPX in the Moffett xenoliths contain an eclogite melt component, then the age of the xenoliths implies that this component must have been present beneath Adak Island in the Holocene.

Coarse CPX in composite xenoliths from Mt. Moffett also commonly show complex and fine-scale patterns of compositional zoning, which may also be interpreted to indicate a young age for these xenoliths. Fig. 3 illustrates oscillations in Mg# for sample 77-43, which is described in detail in Conrad and Kay [7]. Because the groundmass of this volcanic-textured xenolith contains glass which is in apparent textural equilibrium with the cumulate minerals, we infer that the xenolith never fully crystallized [i.e., it was a melt that quenched against the host magma that carried it to the surface, [7]]. This means that CPX in this xenolith have been in the presence of melt within the arc crust since it first crystallized. Assuming that this temperature is no less than 900° C, and using the experimentally determined interdiffusion coefficient of $D_{Fe-Mg} = 1.30 \times 10^{-22}$ m^2/s for diopside at this temperature [70], we estimate that the sharp boundaries of these oscillations, which commonly are no more than ~6 μm thick, must be less than 100,000 years old (Fig. 8). Even if this textural interpretation is not correct, and the xenolith was held within the crust at 800 °C, the diffusion modeling

Table 3
Trace element analyses of clinopyroxenes from Mt. Moffett xenoliths

| Sample no.	MM77-102	MM77-102	MM77-102A	MM77-102A	MM77-102C	MM77-102C	MM77-102C	MM77-43	MM77-43	MM77-43	MM77-43	MM79A	MMDK
Analysis no.	5	1	8	3b	7	8	3	1.3i	1.5i	2.0	3.0	2.2r	3.0
Mg#	0.91	0.89	0.81	0.90	0.91	0.87	0.84	0.91	0.87	0.83	0.79	0.77	0.81
Ti	726	970	1742	698	587	929	1419	753	2266	1535	3345	2777	4056
V	69	120	281	75	67	139	199	97	206	166	299	298	342
Cr	5332	3057	2208	4290	4128	1792	1364	2496	1793	744	792	102	421
Sr	68.5	37.1	51.6	48.2	39.6	39.6	42.1	34.6	40.5	52.6	54.4	35.9	26.0
Y	1.45	2.6	9.3	2.4	1.67	2.6	5.5	2.4	5.47	6.43	10.71	9.28	6.90
Zr	1.81	3.3	16.3	2.1	2.50	2.5	9.6	1.7	9.59	7.09	19.6	14.6	13.3
La	0.25	0.30	0.78	0.44	0.43	0.51	0.66	1.09	1.12	1.19	1.96	0.55	1.57
Ce	1.27	1.33	3.41	1.91	1.56	2.00	2.82	3.67	3.35	3.18	4.41	2.68	5.24
Nd	1.40	1.6	3.7	2.05	1.85	2.08	3.01	4.9	4.47	4.16	6.89	3.22	4.80
Sm	0.53	0.52	1.42	0.90	0.81	0.79	1.13	1.51	1.42	1.43	2.64	1.45	1.83
Eu	0.15	0.18	0.47	0.25	0.22	0.26	0.41	0.59	0.54	0.49	0.81	0.62	0.59
Dy	0.31	0.46	1.33	0.49	0.54	0.56	0.82	1.59	1.36	1.25	2.07	1.76	1.77
Er	0.16	0.24	0.76	0.30	0.31	0.33	0.51	0.80	0.63	0.70	1.13	0.82	0.85
Yb	0.13	0.22	0.65	0.27	0.26	0.31	0.47	0.68	0.60	0.45	0.77	0.82	0.91
Nd/Yb	10.5	7.07	5.78	7.52	7.20	6.63	6.41	7.19	7.48	9.23	8.99	3.91	5.27
Sr/Y	47.2	14.2	5.56	20.3	23.8	15.1	7.68	14.6	7.40	8.18	5.08	3.86	3.76
Nd/Zr	0.77	0.47	0.23	0.98	0.74	0.83	0.31	2.92	0.47	0.59	0.35	0.22	0.36
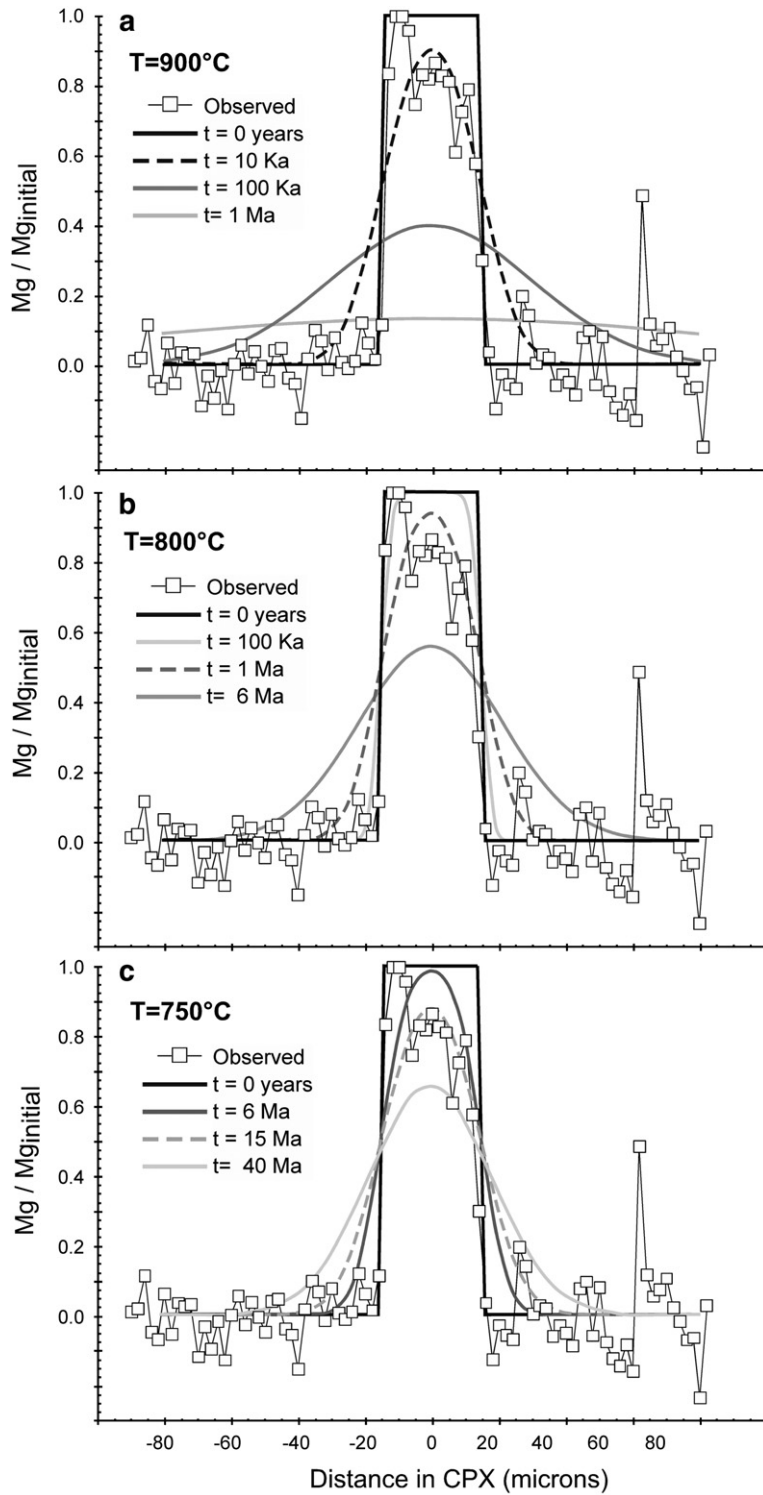
Fig. 8. Results of diffusion modeling, showing one of the observed oscillations in Mg content expressed relative to the maximum Mg content at the height of the Mg# peak (Mg/Mg$_{initial}$). Observed variation shown here (white boxes), which is the same data as in Fig. 3, but with the left-hand peak removed for simplicity, is compared with predicted interdiffusional relaxation of an initially flat-topped peak at $t=0$ years after time periods of 10 ka and to 40 Ma and diffusion coefficients at 900 °C ($D=1.30\times10^{-22}$ m^2/s), 800 °C ($D=1.00\times10^{-24}$ m^2/s) and 750 °C (1.00×10^{-25} m^2/s). The models (show by smooth gray lines) are based on Eq. (2.15) in Crank [84]. Diffusion coefficients from Dimanov and Sautter [70].

indicates that the compositional oscillations must be less than 6 m.y.-old (Fig. 8). At lower temperatures (<750 °C), the storage time could be much longer (>>10 Ma, Fig. 8), nonetheless, the textural evidence and diffusion modeling appear to confirm a young age for the sample #77-43, which contains high-Mg# CPX that have the high Sr/Y geochemical component.

4.3. Tholeiitic and calc–alkaline magmatism

The contrasting nature of the Kanaga and Moffett xenoliths suggests that they formed in magmatic systems that must have evolved along different liquid lines of descent. Considering all aspects of the xenoliths, it seems likely that these evolutionary pathways correspond respectively, to the tholeiitic and calc–alkaline igneous series.

The Kanaga xenoliths appear tholeiitic in the sense that they provide a record of magmatic evolution that would have produced olivine, plagioclase and pyroxene–phyric lavas over a wide range of whole-rock Mg#'s. These evolving magmas were free of amphibole or other hydrous minerals, had relatively flat trace element patterns, showing only modest enrichments relative to MORB, but spanning a wide range of concentration levels (Figs. 5, 6). At high trace element abundances and low Mg#, these magmas maintained relatively flat REE patterns but had pronounced, negative Eu anomalies (Fig. 5). In the Aleutians, lavas such as these are seen in tholeiitic volcanic systems that produce mostly high-Al basalt, and diminishingly smaller volumes of andesite, dacite and rhyodacite [15,71–74]. Plutonic equivalents of these systems also exist, for example in the Finger Bay Pluton [75].

In contrast, the Moffett xenoliths record a magmatic system that produced hornblende-bearing magmas with diverse and enriched trace element patterns (i.e., high and highly variable La/Yb, Sr/Y, etc.). Relatively early crystallization of amphibole and Fe–Ti oxides under hydrous and relatively low-temperature conditions, would have driven these magmas to elevated SiO_2 contents at high Mg#'s. Some primitive magmas in this system may have themselves been andesitic when they entered the crust (53–58% SiO_2), due to the interaction between a silicic, eclogite melts from the subducting plate with peridotite of the mantle wedge [16,18,19,33,76]. Amphibole-oxide crystallization in response to high water contents resulted in a calc–alkaline evolutionary pathway that produced hornblende-bearing andesites and dacites, which would have had relatively low abundances of the middle-and-heavy REE, due to the effects of amphibole fractionation. The REE patterns for these magmas would also have lacked a significant Eu anomaly, probably due to the limited extent of plagioclase crystallization under hydrous and probably oxidizing conditions [32]. Textural features of the Moffett xenoliths, described in detail by Conrad and Kay [7], suggest that even the evolved lavas produced by this system would have contained strongly out-of-equilibrium, high Mg# minerals with complex zoning patterns, giving evidence for magma mixing. Lavas such as these are commonly observed at calc–alkaline volcanic systems in the Aleutians (e.g., [40,77]). Calc–alkaline volcanic systems in the Aleutians are small compared to tholeiitic systems, but calc–alkaline plutonic bodies are comparatively large [19,77,78]. We believe this is because primitive calc–alkaline melts are less likely to erupt because they are comparatively cool, volatile-rich and high in SiO_2 when they arise from the mantle. Such melts will commonly stall and crystallize in the arc crust when they rise to areas of low pressure and lose their volatile components [19,77,78].

Based on the above, we suggest that the contrasting styles of tholeiitic and calc–alkaline volcanism result from differences in the primitive melts entering the crust [19], not the result of divergent evolution from a common primitive magma in crustal-level magma systems [15,77]. This argument for subduction-level control is supported by the observation that magmatic composition in the Aleutians is correlated with regional-scale features such as subduction and melt production rates, and with the physical conditions in the subduction zone, especially the temperature of the mantle wedge compared to that of the subducting plate [19]. All of these features change systematically along the length of the Aleutian arc and are correlated with the volcanic style which is predominantly tholeiitic to the east of the Adak area, and predominantly calc–alkaline from the Adak area westward [19]. Based on this, we speculate that the thermal structure of the mantle wedge may play a role in controlling the locations of tholeiitic versus calc–alkaline volcanoes in the Aleutians. In this kind of model, calc–alkaline volcanoes may be viewed as the cool magmatic products of mantle wedge environments that have been affected by features such as the 'cold plumes' of Gerya and Yuen [79] which, based on geodynamic modeling, can be expected (under some circumstances) to produce mantle-derived magmas that are relatively cool and somewhat enriched with respect to trace element patterns, due to the presence of an eclogite melt component from the subducting oceanic crust [80]. This view suggests that volcano spacing and segmentation of the Aleutian arc, which are often

attributed to local structures within the arc crust [15,77,81], may more appropriately be viewed as products of the thermal structure of the underlying mantle wedge.

5. Conclusions

Trace element geochemistry of CPX in xenoliths from Kanaga Island and from Mt. Moffett on Adak Island, leads to the following conclusions about primitive magma genesis and the physical conditions within the Aleutian subduction zone.

1. Xenoliths collected from (probable) Neogene-age volcanic rocks on Kanaga Island are deformed fragments of the Aleutian plutonic crust which originated as cumulates and cumulate-melt mixtures from melts that were relatively anhydrous and had flat-to-modestly enriched trace element patterns, similar in most ways to those of modern Aleutian basalts. These results largely confirm those of whole-rock studies of the Kanaga xenoliths [22].
2. Xenoliths hosted by Holocene-age pyroclastic deposits from Mt. Moffett on Adak Island are largely undeformed fragments of mafic and ultramafic plutonic rocks that formed from crystallization of primitive melts that had trace element patterns broadly similar to those observed in the geochemically enriched primitive andesites that are common among Miocene-age and younger volcanic rocks in the western Aleutians. These results confirm many aspects of previous studies of these xenoliths [7,25], with the important caveat that the trace element contents of high-Mg# CPX require a parental melt that was geochemically more enriched (higher La/Yb, Sr/Y, etc.) than basaltic lavas like those that are common in the modern Aleutian arc.
3. If the geochemically enriched component in the Moffett xenoliths is formed by melting of the basaltic part of the subducting oceanic crust in the eclogite facies [16,18–20], then it's presence in the subduction zone beneath the Adak area is inconsistent with thermal models that predict melting of the subducting oceanic crust only in places where the oceanic lithosphere is exceptionally young [e.g., less than 10 Ma — [43,82]]. These trace element results are however, consistent with recent thermal models which incorporate temperature-dependent and/or non-Newtonian viscosities.
4. Based on the foregoing we infer that melt evolution along the calc–alkaline and tholeiitic igneous series in the Aleutians is controlled to a large degree, by the physical and chemical characteristics, especially volatile and SiO_2 content, of the primitive melts that are formed in the subduction zone. This conclusion is consistent with the observation that Aleutian volcanism becomes increasingly calc–alkaline from east-to-west along the oceanic part of the arc, apparently in response to changes in subduction rates, which are inferred to control the relative temperature of the subducting plate and mantle wedge sources [19].

References

[1] B.L. Weaver, J. Tarney, Major and trace element composition of the continental lithosphere, Phys. Chem. Earth 15 (1984) 39–68.
[2] S.R. Taylor, S.M. McLennan, The Continental Crust: Its Composition and Evolution, Blackwell Scientific Publishers, 1985, 312 pp.
[3] C.J. Nye, M.R. Reid, Geochemistry of primary and least fractionated lavas from Okmok Volcano, Central Aleutians: implications for arc magmagenesis, J. Geophys. Res. 91 (1986) 10271–10287.
[4] R.J. Stern, J. Morris, S.H. Bloomer, J.W. Hawkins, The source of the subduction component in convergent margin magmas: trace element and radiogenic isotope evidence from Eocene boninites, Mariana forearc, Geochim. Cosmochim. Acta 55 (1991) 1467–1481.
[5] Y. Tatsumi, K. Ishizaka, Origin of high-magnesium andesites in the Setouchi volcanic belt, southwest Japan, I. Petrographical and chemical characteristics, Earth Planet. Sci. Lett. 60 (1982) 293–304.
[6] J. Gill, Orogenic Andesites and Plate Tectonics, Springer-Verlag, New York, 1981, 390 pp.
[7] W.K. Conrad, R.W. Kay, Ultramafic and mafic inclusions from Adak Island: crystallization history, and implications for the nature of primary magmas and crustal evolution in the Aleutian arc, J. Petrol. 25 (1984) 88–125.
[8] A.D. Brandon, D.S. Draper, Constraints on the origin of the oxidation state of mantle overlying subduction zones: an example from Simcoe, Washington, USA, Geochim. Cosmochim. Acta 60 (1996) 1739–1749.
[9] P. Schiano, R. Clocchiatti, N. Shimizu, R.C. Maury, K.P. Jochum, A.W. Hofmann, Hydrous, silica-rich melts in the sub-arc mantle and their relationship with erupted arc lavas, Nature 377 (1995) 595–600.

[10] S.M. DeBari, S.M. Kay, R.W. Kay, Ultramafic xenoliths from Adagdak Volcano, Adak, Aleutian Islands, Alaska: deformed igneous cumulates from the Moho of an island arc, J. Geol. 95 (1987) 329–341.

[11] E. Takahashi, Thermal history of lherzolite xenoliths I: petrology of lherzolite xenoliths from Ichinomegata crater, Oga Peninsula, northeast Japan, Geochim. Cosmochim. Acta 44 (1980) 1643–1658.

[12] S. Arai, S. Takada, K. Michibayashi, M. Kida, Petrology of peridotite xenoliths from Iraya Volcano, Philippines, and its implications for dynamic mantle-wedge processes, J. Petrol. 45 (2004) 369–389.

[13] I.N. Bindeman, J.C. Bailey, Trace elements in anorthite megacrysts from the Kurile Island Arc: a window to across-arc geochemical variations in magma compositions, Earth Planet. Sci. Lett. 169 (1999) 209–226.

[14] G.M. Yogodzinski, P.B. Kelemen, Slab melting in the Aleutians: implications of an ion probe study of clinopyroxene in primitive adakite and basalt, Earth Planet. Sci. Lett. 158 (1998) 53–65.

[15] S.M. Kay, R.W. Kay, G.P. Citron, Tectonic controls on tholeiitic and calc–alkaline magmatism in the Aleutian arc, J. Geophys. Res. 87 (1982) 4051–4072.

[16] R.W. Kay, Aleutian magnesian andesites: melts from subducted Pacific ocean crust, J. Volcanol. Geotherm. Res. 4 (1978) 117–132.

[17] J.D. Myers, B.D. Marsh, Aleutian lead isotopic data: additional evidence for the evolution of lithospheric plumbing systems, Geochim. Cosmochim. Acta 51 (1987) 1833–1842.

[18] G.M. Yogodzinski, R.W. Kay, O.N. Volynets, A.V. Koloskov, S.M. Kay, Magnesian andesite in the western Aleutian Komandorsky region: implications for slab melting and processes in the mantle wedge, Geol. Soc. Amer. Bull. 107 (5) (1995) 505–519.

[19] P.B. Kelemen, G.M. Yogodzinski, D.W. Scholl, Along-strike variation in lavas of the Aleutian Island Arc: implications for the genesis of high Mg# andesite and the continental crust, in: J. Eiler (Ed.), Inside the Subduction Factory, Geophysical Monograph, vol. 138, American Geophysical Union, Washington D.C, 2003, pp. 223–276.

[20] M.J. Defant, M.S. Drummond, Derivation of some modern arc magmas by melting of young subducted lithosphere, Nature 347 (1990) 662–665.

[21] S.E. DeLong, F.N. Hodges, R.J. Arculus, Ultramafic and mafic inclusions, Kanaga Island, Alaska, and the occurrence of alkaline rocks in island arcs, J. Geol. 83 (1975) 721–736.

[22] J.D. Romick, Silicic Volcanism and Granulite Xenoliths from the Aleutian Islands, Alaska: Petrologic Constraints for the Evolution of the Aleutian Arc Crust, Ph.D., Cornell University, 1990.

[23] S.E. Swanson, S.M. Kay, M. Brearley, C.M. Scarfe, Arc and back-arc xenoliths in Kurile–Kamchatka and western Alaska, in: P.H. Nixon (Ed.), Mantle Xenoliths, John Wiley and Sons, New York, 1987, pp. 303–318.

[24] R.R. Pope, The petrology of ultramafic and mafic xenoliths from Kanaga Island, the central Aleutians, Masters, Cornell University, 1983.

[25] W.K. Conrad, S.M. Kay, R.W. Kay, Magma mixing in the Aleutian Arc: evidence from cognate inclusions and composite xenoliths, J. Volcanol. Geotherm. Res. 18 (1983) 279–295.

[26] R.W. Kay, S.M. Kay, Crustal recycling and the Aleutian arc, Geochim. Cosmochim. Acta 52 (1988) 1351–1359.

[27] R.W. Kay, J.L. Rubenstone, S.M. Kay, Aleutian terranes from Nd isotopes, Nature 322 (1986) 605–609.

[28] T. Kawasaki, E. Ito, An experimental determination of the exchange reaction of Fe2+ and Mg2+ between olivine and Ca-rich clinopyroxene, Am. Min. 79 (1994) 461–477.

[29] G.A. Gaetani, T.L. Grove, Partitioning of rare-earth elements between clinopyroxene and silicate melt: crystal–chemical controls, Geochim. Cosmochim. Acta 59 (1995) 1951–1962.

[30] E. Hill, B.J. Wood, J.D. Blundy, The effect of Ca-Tschermaks component on trace element partitioning between clinopyroxene and silicate melt, Lithos 53 (2000) 203–215.

[31] N. Shimizu, The oscillatory trace element zoning of augite phenocrysts, Earth Sci. Rev. 29 (1990) 27–37.

[32] J.D. Romick, S.M. Kay, R.W. Kay, The influence of amphibole fractionation on the evolution of calc–alkaline andesite and dacite tephra from the central Aleutians, Alaska, Contrib. Mineral. Petrol. 112 (1992) 101–118.

[33] G.M. Yogodzinski, O.N. Volynets, A.V. Koloskov, N.I. Seliverstov, V.V. Matvenkov, Magnesian andesites and the subduction component in a strongly calc–alkaline series at Piip Volcano, Far Western Aleutians, J. Petrol. 35 (1) (1994) 163–204.

[34] E. Rose, N. Shimizu, G. Layne, T.L. Grove, Melt production beneath Mt. Shasta from boron data in primitive melt inclusions, Science 293 (2001) 281–283.

[35] M.B. Baker, T.L. Grove, R. Price, Primitive basalts and andesites from the Mt. Shasta region, N. California; products of varying melt fraction and water content, Contrib. Mineral. Petrol. 118 (1994) 111–129.

[36] N. Shimizu, T.L. Grove, Geochemical studies of olivine-hosted melt inclusions from ridges and arcs, Eos 79 (1998) F1002.

[37] T.L. Grove, L.T. Elkins-Tanton, S.W. Parman, N. Chatterjee, O. Müntener, G.A. Gaetani, Fractional crystallization and mantle-meting controls on calc–alkaline differentiation trends, Contrib. Mineral. Petrol. 145 (2003) 515–533.

[38] T.L. Grove, M.B. Baker, T.D. Price, S.W. Parman, L.T. Elkins-Tanton, N. Chatterjee, O. Müntener, Magnesian andesite and dacite lavas from Mt. Shasta, northern California: products of fractional crystallization of H_2O-rich mantle melts, Contrib. Mineral. Petrol. 148 (2004) 542–565.

[39] I.N. Bindeman, J.M. Eiler, G.M. Yogodzinski, Y. Tatsumi, C.R. Stern, T.L. Grove, M. Portnyagin, K. Hoernle, L.V. Danushevsky, Oxygen isotope evidence for slab melting in modern and ancient subduction zones, Earth Planet. Sci. Lett. 235 (2005) 480–496.

[40] J.D. Myers, B.D. Marsh, A.K. Sinha, Strontium isotopic and selected trace element variations between two Aleutian volcanic centers (Adak and Atka): implications for the development of arc volcanic plumbing systems, Contrib. Mineral. Petrol. 91 (1985) 221–234.

[41] P. Lonsdale, Paleogene history of the Kula plate: offshore evidence and onshore implications, Geol. Soc. Amer. Bull. 100 (1988) 733–754.

[42] T. Atwater, Plate tectonic history of the northeast Pacific and western North America, in: E.L. Winterer, D.M. Hussong, R.W. Decker (Eds.), The Eastern Pacific Ocean and Hawaii: The Geology of North America, Geological Society of America, Boulder, 1989, pp. 21–72.

[43] S.M. Peacock, Numerical simulation of subduction zone pressure–temperature–time paths: constraints on fluid production and arc magmatism, Philos. Trans.: Phys. Sci. Eng. 335 (1638) (1991) 341–353.

[44] S.M. Peacock, T. Rushmer, A.B. Thompson, Partial melting of subducting oceanic crust, Earth Planet. Sci. Lett. 121 (1994) 227–244.

[45] J.H. Davies, D.J. Stevenson, Physical model of source region of subduction zone volcanics, J. Geophys. Res. 97 (1992) 2037–2070.

[46] H. Iwamori, Heat sources and melting in subduction zones, J. Geophys. Res. 102 (1997) 14803–14820.

[47] J.H. Davies, The role of hydraulic fractures and intermediate-depth earthquakes in generating subduction-zone magmatism, Nature 398 (1999) 142–145.

[48] P.B. Kelemen, J.L. Rilling, E.M. Parmentier, L. Mehl, B.R. Hacker, Thermal structure due to solid-state flow in the mantle wedge beneath arcs, in: J. Eiler (Ed.), Inside the Subduction Factory, Geophysical Monograph, vol. 138, American Geophysical Union, Washington D.C., 2003, pp. 293–311.

[49] P.E. van Keken, B. Kiefer, S.M. Peacock, High-resolution models of subduction zones: implications for mineral dehydration reactions and the transport of water into the deep mantle 2002, Geochem. Geophys. Geosys. (2002).

[50] J.A. Conder, A case for hot slab surface temperatures in numerical viscous flow models of subduction zones with an improved fault zone parameterization, Phys. Earth Planet. Inter. 149 (2005) 155–164.

[51] M.W. Schmidt, D. Vielzeuf, E. Auzanneau, Melting and dissolution of subducting crust at high pressures: the key role of white mica, Earth Planet. Sci. Lett. 228 (2004) 65–84.

[52] G.T. Nichols, P.J. Wyllie, C.R. Stern, Subduction zone melting of pelagic sediments constrained by melting experiments, Nature 371 (1994) 785–788.

[53] G.T. Nichols, P.J. Wyllie, C.R. Stern, Phase equilibria constraints on models of subduction zone magmatism, Subduction Top to Bottom, Geophysical Monograph, vol. 96, American Geophysical Union, Washington D.C., 1996, pp. 293–298.

[54] I.B. Lambert, P.Y. Wyllie, Melting of gabbro (quartz eclogite) with excess water to 35 kilobars, with geological applications, J. Geol. 80 (1972) 693–708.

[55] C.R. Stern, P.J. Wyllie, Melting relations of basalt–andesite–rhyolite H_2O and a pelagic red clay at 30 kb, Contrib. Mineral. Petrol. 42 (1973) 313–323.

[56] T. Plank, C.H. Langmuir, The chemical composition of subducting sediment and its consequences for the crust and mantle, Chem. Geol. 145 (1998) 325–394.

[57] T. Plank, C.H. Langmuir, Tracing trace elements from sediment input to volcanic output at subduction zones, Nature 362 (1993) 739–742.

[58] T. Plank, Constraints from Thorium/Lanthanum on sediment recycling at subduction zones and the evolution of continents, J. Petrol. 46 (2005) 921–944.

[59] T. Elliott, T. Plank, A. Zindler, W. White, B. Bourdon, Element transport from slab to volcanic front at the Mariana arc, J. Geophys. Res. 102 (1997) 14,991–15,019.

[60] C.J. Hawkesworth, K. Gallagher, J.M. Hergt, F. McDermott, Trace element fractionation processes in the generation of island arc basalts, Philos. Trans. R. Soc. Lond., A 342 (1993) 179–191.

[61] C.J. Hawkesworth, K. Gallagher, J.M. Hergt, F. McDermott, Mantle and slab contributions in arc magmas, Annu. Rev. Earth Planet. Sci. 21 (1993) 175–204.

[62] C. Class, D.M. Miller, S.L. Goldstein, C.H. Langmuir, Distinguishing melt and fluid subduction components in Umnak Volcanics, Aleutian Arc, Geochem. Geophys. Geosys. (2000).

[63] R. Kessel, M.W. Schmidt, P. Ulmer, T. Pettke, Trace element signature of subduction-zone fluids, melts and supercritical liquids at 120–180 km depth, Nature 437 (2005) 724–727.

[64] R. Kessel, P. Ulmer, T. Pettke, M.W. Schmidt, A.B. Thompson, The water-basalt system at 4 to 6 GPa: Phase relations and second critical endpoint in a K-free eclogite at 700 to 1400 °C, Earth Planet. Sci. Lett. 237 (2005) 873–792.

[65] J.M. Brenan, H.F. Shaw, D.L. Phinney, R.F.J., Rutile — aqueous fluid partitioning of Nb, Ta, Hf, Zr, U and Th: implications for high field strength element depletions in island-arc basalts, Earth Planet. Sci. Lett. 128 (1994) 327–339.

[66] J.M. Brenan, H.F. Shaw, R.J. Ryerson, D.L. Phinney, Mineral — aqueous fluid partitioning of trace elements at 900 °C and 2.0 GPa: Constraints on trace element chemistry of mantle and deep crustal fluids, Geochim. Cosmochim. Acta 59 (1995) 3331–3350.

[67] T.H. Green, J. Adam, Experimentally determined characteristics of aqueous fluid from partially dehydrated mafic oceanic crust at 3.0 GPa, 650°–700 °C, Eur. J. Mineral. 15 (2003) 815–830.

[68] Y. Tatsumi, D.L. Hamilton, R.W. Nesbitt, Chemical characteristics of fluid phase released from a subducted lithosphere and origin of arc magmas: evidence from high-pressure experiments and natural rocks, J. Volcanol. Geotherm. Res. 29 (1986) 293–309.

[69] R.W. Kay, S.M. Kay, P. Layer, Original Aleutian Adakite dated at 11.8 Ma; slab melt thermal dilemma resolved? Eos 79 (1998) F396.

[70] A. Dimanov, V. Sautter, "Average" interdiffusion of (Fe, Mn)–Mg in natural diopside, Eur. J. Mineral. 12 (2000) 749–760.

[71] B.S. Singer, J.D. Myers, C.D. Frost, Mid-Pleistocene lavas from the Seguam volcanic center, central Aleutian arc: closed-system fractional crystallization of a basalt to rhyodacite eruptive suite, Contrib. Mineral. Petrol. 110 (1992) 87–112.

[72] B.S. Singer, J.D. Myers, C.D. Frost, Mid-Pleistocene basalts from the Seguam Volcanic Center, Central Aleutian arc, Alaska: local lithospheric structures and source variability in the Aleutian arc, J. Geophys. Res. 97 (1992) 4561–4578.

[73] D.M. Miller, C.H. Langmuir, S.L. Goldstein, A.L. Franks, The importance of parental magma composition to calc–alkaline and tholeiitic evolution: evidence from Umnak Island in the Aleutians, J. Geophys. Res. 97 (1992) 321–343.

[74] S.M. Kay, R.W. Kay, Aleutian magmas in space and time, in: G. Plafker, H.C. Berg (Eds.), The Geology of Alaska, The Geology of North America, vol. G-1, Geological Society of America, Boulder, 1994, pp. 687–722.

[75] S.M. Kay, R.W. Kay, H.K. Brueckner, J.L. Rubenstone, Tholeiitic Aleutian Arc plutonism: the Finger Bay Pluton, Adak, Alaska, Contrib. Mineral. Petrol. 82 (1983) 99–116.

[76] R.P. Rapp, N. Shimizu, M.D. Norman, G.S. Applegate, Reaction between slab-derived melts and peridotite in the mantle wedge: experimental constraints at 3.8 GPa, Chem. Geol. 160 (1999) 335–356.

[77] S.M. Kay, R.W. Kay, Aleutian tholeiitic and calc–alkaline magma series I: the mafic phenocrysts, Contrib. Mineral. Petrol. 90 (1985) 276–290.

[78] S.M. Kay, R.W. Kay, M.R. Perfit, Calc–alkaline plutonism in the intra-oceanic Aleutian arc, Alaska, in: S.M. Kay, C.W. Rapela (Eds.), Plutonism from Antarctica to Alaska: Geological Society of America Special Paper, vol. 241, 1990, pp. 233–255, Boulder.

[79] T.V. Gerya, D.A. Yuen, Rayleigh–Taylor instabilities from hydration and melting propel 'cold plumes' at subduction zones, Earth Planet. Sci. Lett. 212 (2003) 47–62.

[80] T.V. Gerya, D.A. Yuen, E.O.D. Sevre, Dynamical causes for incipient magma chambers above slabs, Geology 32 (2004) 89–92.

[81] E.L. Geist, J.R. Childs, D.W. Scholl, The origin of summit basins of the Aleutian Ridge: implications for block rotation of an arc massif, Tectonics 7 (1988) 327–341.

[82] S.M. Peacock, Thermal and petrologic structure of subduction zones, in: G.E. Bebout, D.W. Scholl, S.H. Kirby, J.P. Platt (Eds.),

Subduction Zones, Top to Bottom: Geophysical Monograph, vol. 96, American Geophysical Union, Washington D.C., 1996, pp. 119–133.

[83] H.J.B. Dick, H.R. Naslund, Late-stage melt evolution and transport in the shallow mantle beneath the East Pacific Rise, in: C. Mével, K.M. Gillis, J.F. Allan, P.S. Meyer (Eds.), Proc. ODP Sci. Results, vol. 147, Ocean Drilling Program, College Station, TX, 1996, pp. 103–134.

[84] J. Crank, The Mathematics of Diffusion, Oxford University Press, London, 1975, 414 pp.